Laser Frequency Jitter Tolerance and Linewidth Requirement for ≥ 64Gbaud DP-16QAM coherent systems

Rui Zhang[1], Wen-Jr Jiang[2], Konstantin Kuzmin[2], Reggie Juluri[2], Gee-Kung Chang[1], and Winston I. Way[2]
(1) School of Electrical and Computer Engineering, Georgia Institute of Technology, Atlanta, GA 30332, USA
(2) NeoPhotonics, 3081 Zanker Road, San Jose, CA 95134, USA
Email: ruizhangece@gatech.edu

Abstract: Equalization-enhanced phase noise-dominated optical carrier frequency jitter tolerance and linewidth requirement for ≥ 64Gbaud DP-16QAM dispersion-unmanaged coherent systems have been investigated. The implication to future 100 Gbaud systems is delineated.
OCIS codes: (060.1660) Coherent communications; (060.3510) Lasers, fiber; (060.2330) Fiber optics communications.

1. Introduction

Clock timing jitter causes bit-errors in all digital communication systems. In these systems, a sinusoidal jitter is usually used to test receiver jitter tolerance, which is essentially a mask based on the allowable peak-to-peak jitter amplitude as a function of jitter frequency. On the other hand, in an optical coherent system with significant fiber chromatic dispersion (CD), a sinusoidal frequency jitter in a local oscillator (LO) laser can cause timing error and irrecoverable inter-symbol-interference-induced bit-errors after CD equalization in a receiver digital signal processor (DSP) [1-3]. This phenomenon is termed equalization enhanced phase noise (EEPN), which applies to both white frequency noise and sinusoidal interference [1-3]. In practice, sinusoidal jitter source originates from switching power supplies and power converters, circuit board, supply voltage variation, and mechanical vibrations [4-6].

In this paper, we investigate not only the LO frequency jitter tolerance in a 32 and 64Gbaud DP-16QAM coherent receiver via experiments and simulations, but also analyze the combined impact of LO linewidth (measured based on the white frequency noise spectral density) and LO frequency sinusoidal jitter with a symbol rate up to 100Gbaud. We limit our study to DP-16QAM, which gives the best compromise between the total data rate and achievable distance [7]. The white frequency noise serves as background noise for the sinusoidal jitter. Thus the lower the laser linewidth, the more tolerant is the coherent receiver to LO frequency jitter, and the longer the transmission distance.

2. Experimental and simulation results

Figure 1 shows the 64-Gbaud DP-16QAM experimental setup. Both the transmitter and LO external cavity lasers (ECLs) had an intrinsic linewidth of 35 KHz and operated at a frequency around 193.5 THz. Four uncorrelated pseudo-random bit sequences (PRBS) with a pattern length of 2^{15} were loaded to four 64 GSa/s digital to analog converters (DACs), i.e., the DACs operated at 1 Sa/symbol. The outputs of the DACs were used to modulate a coherent driver modulator (CDM), whose 3dB bandwidth was 40 GHz and Vπ was 2V. A CD emulator with an 8-dB insertion loss was used to emulate the total CD of 450 or 900 km standard single-mode fiber (SSMF). Comparing to using SSMF spools and in-line EDFAs, the CD emulator completely removes the concern of mixing fiber nonlinearity in the study. At the receiver side, a phase modulator and a low-speed arbitrary waveform generator were used to modulate the LO with a sinusoidal tone. After the intradyne coherent receiver (ICR), a 4-channel 80-GSa/s real-time scope captures the data at 1.25 Sa/symbol. The receiver DSP structure is shown on the right of Figure 1. The data is resampled to 2 Sa/symbol, orthonormalized using Gram-Schmidt orthogonalization procedure, followed by CD compensation and skew estimation, a 64-tap adaptive equalizer, carrier frequency offset (CFO) estimation, and blind-phase search (BPS) carrier phase recovery (CPR).

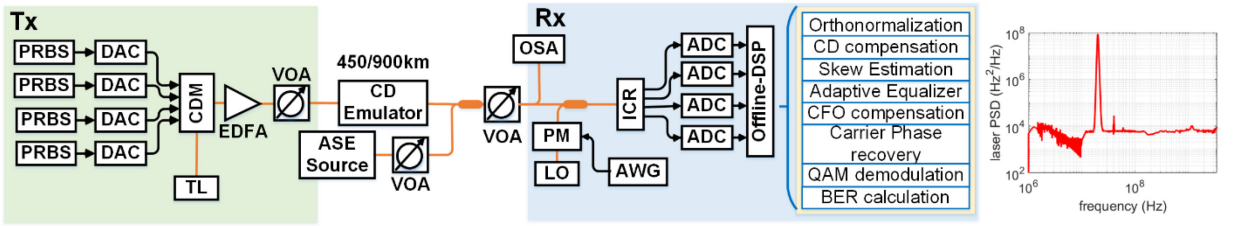

Fig 1. Experimental setup of the 64/32-Gbaud DP 16QAM coherent transmission. TL: Tunable laser, CDM: coherent driver modulator, DAC: digital-to-analog convertor, EDFA: Erbium-doped fiber amplifier, OSA: optical spectrum analyzer, PM: phase modulator, ICR: Intradyne coherent receiver. Inset: Frequency noise PSD of the phase modulated LO with a 20 MHz tone and Δf_{pp} = 80 MHz.

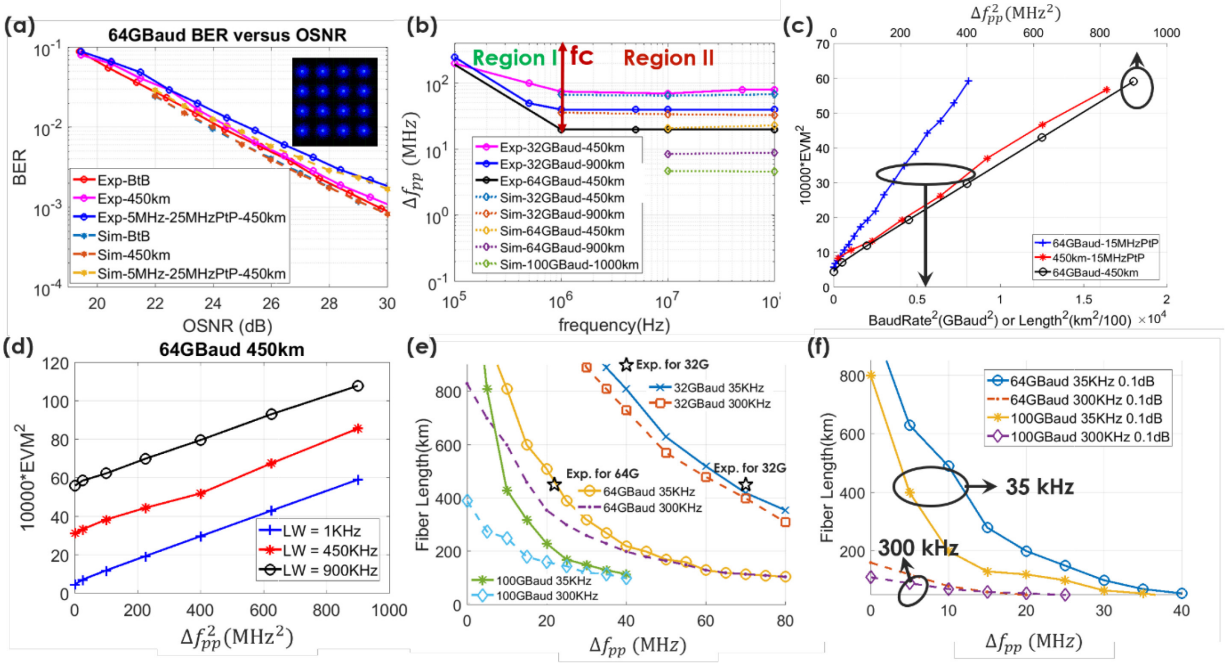

Fig 2. Experimental and simulation results of (a) the BER versus OSNR. (rec. opt. power= -8dBm) for 64-Gbaud DP-16QAM BtB/450-km transmission with a 5-MHz sinusoidal tone and Δf_{pp}=25MHz causing 0.8dB OSNR penalty, (b) Single sinusoidal jitter tolerance versus sinusoidal frequency, at 0.5dB rOSNR penalty, for various baud rates and distances. (c) EVM^2 versus $\Delta f_{pp}{}^2$, (fiber length)^2, and (baud rate)^2, with laser linewidth =1 kHz. (d) EVM^2 versus single tone $\Delta f_{pp}{}^2$ with different laser linewidths. Fiber reach versus Δf_{pp} with 35 and 300 kHz intrinsic linewidth for (e) 0.5-dB penalty at BER = 1e-2 in 32/64/100-Gbaud DP-16QAM transmission, and (f) 0.1-dB penalty at BER = 1e-2 in 64/100-Gbaud DP-16QAM transmission.

Figure 2 (a) shows the 64Gbaud DP-16QAM bit error rate (BER) versus optical signal to noise ratio (OSNR) for back-to-back and 450-km transmission after adding to the LO a 5-MHz sinusoidal jitter source with a peak-to-peak frequency deviation Δf_{pp}= 25 MHz, which caused a 0.8-dB required optical signal to noise ratio (rOSNR) penalty at BER= 1e-2. The experimental and simulation results match very well. This established our baseline for both experiment and simulation. Next, in order to obtain the LO frequency jitter mask, we swept the frequency and Δf_{pp} of the sinusoidal tone to get a 0.5-dB rOSNR penalty at BER = 1e-2 in both the experiment and simulation. The resultant frequency jitter mask is shown in Fig.2 (b), which includes 32Gbaud DP-16QAM so that we can observe the trend- we can see that the mask gets tighter with increasing baud rate and transmission distance. For 32-Gbaud 450-km transmission, the maximum Δf_{pp} is 70 MHz while it is reduced to 40 MHz when the transmission distance is increased to 900-km. For the 64-Gbaud transmission, the maximum Δf_{pp} is reduced from 21 MHz to 8.5 MHz when the distance is extended from 450-km to 900-km. The mask floor is further reduced to 4.7 MHz for 100 Gbaud and 1000 km. Note that the frequency jitter mask is divided into two regions by a corner frequency f_c, which is inversely proportional to the block length of the CFO compensation. The slow frequency drift in region I does not affect laser lineshape and is handled by the CFO compensation section in DSP, while the faster frequency jitter in region II affects the laser lineshape and results in phase variance as well as EEPN [1]. The phase variance is handled by the BPS CPR section in DSP. However, EEPN cannot be mitigated by CPR. As shown in Fig.2(b), the frequency jitter tolerance in region II is obviously much tighter than that of region I. Therefore, the frequency jitter in region II dominates the system performance. Note that the frequency jitter mask in region I is not only determined by Δf_{pp}, but

also by the initial phase of the sinusoidal tone [1,4]. Hence, we have swept the initial phase of the sinusoidal tone to obtain the tightest jitter tolerance in the experiment.

3. Combined effect of LO frequency jitter and laser linewidth

In a coherent system, when laser relative intensity noise (RIN) and any amplitude fluctuation are ignored, the electrical field $E(t)$ with a sinusoidal jitter tone can be modeled as [4]:

$$E(t) = A\exp\left(j\left(\omega_c t + \Delta f_{pp}/(2f_t)\cdot\cos(2\pi f_t t) + n_w(t)\right)\right) \quad (1)$$

where A is the amplitude, ω_c is the laser carrier frequency, Δf_{pp} and f_t are the peak-to-peak frequency deviation and the frequency of the sinusoidal jitter tone, and $n_w(t)$ is the white frequency noise that is related to the laser linewidth. The square of error vector magnitude (EVM) due to laser linewidth-induced EEPN has been shown to be proportional to fiber length (L), baud rate ($1/Ts$) and laser linewidth (LW) [1-3]:

$$EVM_1^2 \propto L\cdot LW/T_s \quad (2)$$

Based on our theoretical analysis and numerical simulations, the square of EVM induced by LO frequency jitter located in region II of Fig.2(b) is proportional to the square of ($\Delta f_{pp} \times L \times$ baud rate), and the simulation results demonstrate this proportionality as shown in Fig.2(c):

$$EVM_2^2 \propto L^2\cdot\Delta f_{pp}^{\ 2}/T_s^2 \quad (3)$$

In Fig. 2(c), all results were obtained for a 64Gbaud DP-16QAM system. EVM^2 versus L^2 is obtained with the Δf_{pp} = 15 MHz, EVM^2 versus baud rate^2 is with Δf_{pp} = 15 MHz and L = 450 km, and EVM^2 versus $\Delta f_{pp}^{\ 2}$ is presented with 450-km transmission. Figure 2(d) shows the simulation results of EVM^2 versus $\Delta f_{pp}^{\ 2}$ for three different laser linewidths of 1, 450, and 900 kHz, which proves that EVM_1 (due to laser linewidth) and EVM_2 (due to LO frequency jitter) are additive. Therefore, the combined effect can be written as:

$$EVM_{total}^{\ 2} \propto L\cdot LW/T_s + \alpha\cdot L^2\cdot\Delta f_{pp}^{\ 2}/T_s^2 \quad (4)$$

where α is an empirical coefficient which can be obtained from the numerical analysis. We have analytically proven that α is independent of the system parameters such as baud rate, fiber length and Δf_{pp}. To examine the combined effect of laser linewidth and LO frequency jitter tone, Fig.2(e) shows the fiber distance (at which a 0.5dB EEPN-induced OSNR penalty is incurred at BER=1e-2) versus Δf_{pp} for 32, 64 and 100 Gbaud DP-16QAM with different laser linewidths. The experimental results for 32 and 64 Gbaud DP-16QAM 450/900km transmission are also included, which match well with the simulation results. Fig.2(f) replaces Fig.2(e) when the EEPN-induced OSNR penalty is reduced from 0.5 to 0.1dB. It is interesting to note that in Fig.2(f), the result matches closely with the OIF 400ZR's laser linewidth specification (in which no OSNR penalty is allocated to laser linewidth) when Δf_{pp}=0. However, in a multi-span transmission system, it would be difficult to separate the EEPN-induced OSNR penalty from the total OSNR penalty, which often contains fiber nonlinearity-induced penalty. Nevertheless, several interesting facts can be observed from Figures 2(e) and 2(f): (i) The transmission distance decreases faster for the smaller Δf_{pp}, and less so for the larger Δf_{pp}, which implies the higher sensitivity of transmission distance to in the smaller LO frequency jitter range. Judging from Fig.2(b), to limit the OSNR penalty to 0.5 dB, Δf_{pp} should not exceed 4.7 ~ 21MHz for ≥ 64Gbaud DP-16QAM, depending on transmission distances and baud rates. (ii) 35KHz laser linewidth provides significantly more margin than that of 300 kHz linewidth in terms of longer transmission distance. For instance, Fig.2(e) shows that for 100Gbaud DP-16QAM transmission, with Δf_{pp} equals to 5 MHz, 35 kHz linewidth extends the 300KHz linewidth's reach of 250 km to 800 km. (iii) The higher the baud rate, the shorter the transmission distance, which implies when the transmission baud rate is increased beyond 100Gbaud, laser linewidth close to or even lower than 35KHz would be required.

In practice, multiple frequency jitter tones could occur, which would result in a scaled down frequency jitter mask, or a tighter requirement on laser linewidth.

4. Conclusions

Via linear system experiments and simulations, we have found that, while EVM^2 due to EEPN is proportional to (baud rate×LO linewidth×L) when considering only the laser linewidth effect, it is proportional to (baud rate×Tone Peak-to-peak frequency drift×L)^2 when considering the sinusoidal frequency jitter effect. This system performance sensitivity to LO sinusoidal frequency jitter indicates the importance of using the jitter tolerance mask shown in Fig.2(b), and its extension to >100Gbaud and >1000km, to qualify tunable lasers. Moreover, due to the additive effect of laser linewidth and sinusoidal frequency jitter, it is expected that a narrower laser linewidth would provide a higher margin for LO frequency jitter tolerance.

5. References

[1] A. Kakkar, *et al*., Scientific Reports, vol. 7, p. 844, 2017.
[2] A. Kakkar, *et al*., Journal of Lightwave Technology, vol. 33, pp. 4834-4841, 2015.
[3] W. Shieh, *et al.*, Opt. Express 16, 15718-15727, 2008.
[4] W. Ng, *et al.*, IEEE Photonics Technology Letters, vol. 26, pp. 486-489, 2014.
[5] M. Kuschnerov, *et al*., IEEE Photonics Technology Letters, vol. 22, pp. 1114-1116, 2010.
[6] J. E. Simsarian, *et al*., IEEE Photonics Technology Letters, vol. 26, pp. 813-816, 2014.
[7] M. Nakamura, *et al*., OFC 2018, M1C.3.